Chaos

Feed-forward artificial neural network provides data-driven inference of functional connectivity

Cite as: Chaos 29, 091101 (2019); https://doi.org/10.1063/1.5117263
Submitted: 30 June 2019 . Accepted: 10 August 2019 . Published Online: 05 September 2019

Nikita Frolov, Vladimir Maksimenko, Annika Lüttjohann, Alexey Koronovskii, and Alexander Hramov

Chaos ARTICLE scitation.org/journal/cha

Feed-forward artificial neural network provides data-driven inference of functional connectivity

Cite as: Chaos **29**, 091101 (2019); doi: 10.1063/1.5117263
Submitted: 30 June 2019 · Accepted: 10 August 2019 ·
Published Online: 5 September 2019

View Online Export Citation CrossMark

Nikita Frolov,[1] Vladimir Maksimenko,[1] Annika Lüttjohann,[2] Alexey Koronovskii,[3] and Alexander Hramov[1,a)]

AFFILIATIONS

[1]Neuroscience and Cognitive Technology Laboratory, Center for Technologies in Robotics and Mechatronics Components, Innopolis University, 420500 Innopolis, The Republic of Tatarstan, Russia
[2]Institute of Physiology I, University of Münster, Münster 48149, Germany
[3]Faculty of Nonlinear Processes, Saratov State University, 410012 Saratov, Russia

[a)]**Electronic mail:** a.hramov@innopolis.ru

ABSTRACT

We propose a new model-free method based on the feed-forward artificial neuronal network for detecting functional connectivity in coupled systems. The developed method which does not require large computational costs and which is able to work with short data trials can be used for analysis and reconstruction of connectivity in experimental multichannel data of different nature. We test this approach on the chaotic Rössler system and demonstrate good agreement with the previous well-known results. Then, we use our method to predict functional connectivity thalamo-cortical network of epileptic brain based on ECoG data set of WAG/Rij rats with genetic predisposition to absence epilepsy. We show the emergence of functional interdependence between cortical layers and thalamic nuclei after epileptic discharge onset.

Artificial neural networks (ANNs) are known to be a powerful tool for big data processing and classification. They are widely used in computer science, nonlinear dynamics, robotics, and neuroscience for solving tasks of classification, forecasting, pattern recognition, etc. In neuroscience, ANNs allow recognizing specific forms of brain activity from multichannel electro- (EEG) or magnetoencephalographic (MEG) data and, therefore, widely used as a computational core in different brain-computer interfaces. Another challenging problem is the analysis of connectivity structures in big multivariate data. In particular, in neuroscience, predicting the functional brain network using multichannel EEG/MEG signals uncovers mechanisms of neuronal interaction during various physiological or cognitive processes. In this report, we use recent advances in the area of machine learning known as feed-forward artificial neuronal network to formulate a method for detecting functional dependence in unidirectionally and bidirectionally coupled systems without additional information about them. We test our mathematical approach on the model coupled chaotic systems and demonstrate good agreement with the previous well-known results on generalized synchronization. Then, we apply our method for the first time to reveal functional connectivity structure in the thalamo-cortical network of epileptic brain based on a rodent ECoG data set.

I. INTRODUCTION

Brain, being one of the most complex systems in nature, exhibits well-pronounced network properties on both anatomical and functional levels.[1–3] The latter implies the existence of functional dependence between the states of remote brain areas, which is believed to provide mechanisms for neuronal communication and information transfer within a distributed brain network. According to the recent theories,[4–8] neural interaction between distant brain regions through emergent functional connectivity structures determines normal brain functioning, including cognitive, motor-related activity, etc. At the same time, abnormalities in functional brain networks stand behind various types of brain disorders like epilepsy, Parkinson's and Alzheimer's diseases, brain tumors, etc.[9,10] Thus, prediction of functional connectivity between brain areas is a crucial approach for brain functioning diagnostics in modern neuroscience.[11]

In nonlinear dynamics, the presence of a functional relation between the dynamics of coupled chaotic systems is known as a particular type of synchronous behavior called "generalized synchronization" (GS).[12–15] This relation may be very complicated, and its explicit form cannot be found in most cases. Recently, the phenomenon of GS has been an object of extensive research, having both theoretical and applied significance (e.g., for information transmission by means of chaotic signals[16–18]).

The definition of the GS regime in the case of unidirectional coupling accepted hitherto is the presence of a functional relation

$$\mathbf{y}(t) = \mathbf{F}(\mathbf{x}(t)) \tag{1}$$

between the drive $\mathbf{x}(t)$ and response $\mathbf{y}(t)$ oscillator states. In Ref. 14, this definition has been generalized on mutual coupling systems as

$$\mathbf{F}(\mathbf{x}(t), \mathbf{y}(t)) = 0. \tag{2}$$

The concept of GS may be essentially applied in neuroscience for data-driven functional connectivity reconstruction based on multichannel EEG/MEG data. However, it has not been systematically used in this context so far. This is due to a number of substantial limitations of existing techniques for detecting the presence of GS in neurophysiological data, which is usually characterized by short duration of time series under analysis, the presence of artifacts and a high level of noise.[19,20] Actually, the most easy, clear, and powerful auxiliary system approach[21] is applicable only for systems with unidirectional coupling and requires the consideration of an identical replica of the response system, which is possible in extremely rare cases. The Lyapunov exponent calculation[14,22] is also effective only for model systems with known model equations for which it is possible to calculate the spectrum of Lyapunov exponents. Finally, the nearest-neighbor method[12,14,23] is a convenient one for GS inference from experimental data, but this approach requires long time series for statistical measure estimation in the phase space.

Motivated by the above discussion, in this report, we develop a model-free data-driven approach for detecting functional dependency inspired by the concepts of nonlinear dynamics and based on feed-forward (FF) artificial neuronal network (ANN). Machine learning techniques are the "cutting edge" of modern big data analysis. Currently, machine learning techniques are widely applied for the analysis and prediction of nonlinear systems dynamics.[24–26] In particular, reservoir computing is used for data-driven model-free estimation of the Lyapunov exponents[27] and for attractor reconstruction[28] of chaotic processes, multilayer perceptron (MLP) detects the nonlinear process of decision-making in the human brain,[29] etc. Recently, Ibáñez-Soria *et al.*[30] applied echo state networks for the detection of functional interrelations in terms of GS. In their work, they stated that architecture of feed-forward neural networks "[…] is suitable for the analysis of stationary problems but, in general, is not adequate to deal with dynamical time-dependent problems." Thus, their approach relied on a recurrent neural network (RNN) to provide the fading memory that allows processing dynamical signals. This approach required the extensive calculations for RNN training and relatively long time series for training and validation.

On the contrary, a new developed method shows that FF MLP-based networks, which are less computationally expensive and able to work with short data trials, are efficient in functional connectivity inference as well. Based on the approximation theorem, MLP with nonlinear activators in hidden layers is able to approximate any arbitrary given function.[31,32] FF MLP may also approximate any function mapping from any finite dimensional discrete space to another.[33] This property of FF MLP is especially useful for the approximation of the functional relation $\mathbf{F}$ in (1) considering only an experimental data set of $\mathbf{x}(t_i)$ and $\mathbf{y}(t_i)$, where $t_i = i\Delta t$ is the discrete time moments and Δt is the sample rate.

II. FEED-FORWARD ANN APPROACH

ANN is known to be a biologically inspired computational system, whose main purpose is to fit unknown and usually complex relationship between input and output data.[33] Since functional connectivity in coupled systems implies the existence of functional dependence between them, ANN seems to be an essential tool in this context.

Figure 1 gives a schematic illustration of the proposed ANN-based method for data-driven functional connectivity detection. Considering two coupled processes, whose dynamics is represented by multivariate signals $\mathbf{x}(t)$ and $\mathbf{y}(t)$, functional connectivity implies $\mathbf{y}(t) = \mathbf{F}(\mathbf{x}(t))$. Since from a mathematical point of view ANN defines a function $f : \mathbf{x} \to \mathbf{y}$, one may use ANN to build a model of the unknown relation $\mathbf{F}(\bullet)$ and predict the $\mathbf{y}$ state based on the $\mathbf{x}$ state. Thus, if a true functional relation $\mathbf{y}(t) = \mathbf{F}[\mathbf{x}(t)]$ exists, ANN is able to approximate it and give a precise prediction $\mathbf{y}'(t)$ of the $\mathbf{y}(t)$ state on the basis of $\mathbf{x}(t)$. On the contrary, if functional dependence is not established, ANN fails to learn it and, therefore, is not able to predict the $\mathbf{y}$-state accurately enough. Summarizing the above, the criterion for functional connectivity inference is equality of predicted and actual values of $\mathbf{y}$ processes: $\mathbf{y}'(t) = \mathbf{y}(t)$.

As compared to a recent paper on the application of echo-state networks (ESNs) to detect GS,[30] our approach does not take into account systems behavior in time domain but verifies the possibility for one-to-one mapping $\mathbf{F} : \mathbf{x} \to \mathbf{y}$. Thus, our method is not subjected to reproducing a systems replicas with exactly the same

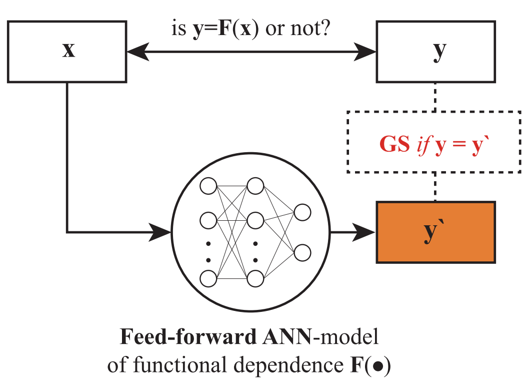

FIG. 1. Inference of functional connectivity using the proposed feed-forward ANN-based approach. Dependence of $\mathbf{y}$ on $\mathbf{x}$ is detected if the ANN-model of functional relation $F(\bullet)$ provides accurate prediction $\mathbf{y}'(t)$ of $\mathbf{y}(t)$-state by the $\mathbf{x}(t)$-state.

dynamical properties using networks with internal memory, and, therefore, requires a more simple architectures of the ANN. In many cases, deep ANNs provide high approximation accuracy and reduce the number of nodes required for the representation of the desired function (see Ref. 33). So, to achieve satisfying result one should carefully set ANN architecture, considering its depth, i.e., the number of hidden layers, as an important parameter. In particular, throughout this study we use the traditional FF ANN architecture—multilayer perceptron. MLP consists of 2 hidden layers, each containing 10 softmax units. The number of both inputs and outputs is determined by the embedding dimensions of coupled systems. Output artificial neurons have a linear activation function.

To infer functional dependence, we consider a pair of multivariate data trials collected from interacting systems $\mathbf{x} = \{\mathbf{x}(t_1), \mathbf{x}(t_2), \ldots, \mathbf{x}(t_N)\}$ and $\mathbf{y} = \{\mathbf{y}(t_1), \mathbf{y}(t_2), \ldots, \mathbf{y}(t_N)\}$, where N is the trial length. Each sample $\mathbf{x}(t_i)$ is assigned a sample $\mathbf{y}(t_i)$, so $\mathbf{x}(t_i)$ is considered as the input data and $\mathbf{y}(t_i)$ as the target data. Then, the data are normalized in the range of $[0, 1]$, shuffled and separated equally into training and validation sets. To train the network, we use an Adam optimizer with a learning rate of 0.001 implemented in the Keras API.[34] To avoid possible fails related with model overfitting, we check the divergence between trainig and validation errors—if these values diverge for the past 10 training epochs, the process is terminated and starts over. To quantify the degree of functional dependence, we use a metric called R^2-score (coefficient of determination), which evaluates "goodness of fit" of the original data collected from a response system $\mathbf{y}(t)$ and its ANN prediction $\mathbf{y}'(t)$ and is defined as

$$R^2 = 1 - \frac{\sum_{d=1}^{D}\sum_{i=1}^{N}\left(y_d(t_i) - y'_d(t_i)\right)^2}{\sum_{d=1}^{D}\sum_{i=1}^{N}\left(y_d(t_i) - \bar{y}_d\right)^2}, \tag{3}$$

where D is the number of dimensions, N is the length of the data set, overbar denotes mean value, $y_d(t)$ and $y'_d(t)$ are the dth component of response system vector state $\mathbf{y}(t)$, and its prediction via ANN, respectively. R^2 ranges from 0 to 1 and quantifies the fraction of data being well predicted by the ANN model. As $R^2 = 0.5$ indicates that only a half of data are fitted by the model (almost random prediction), this value is further considered as a threshold value for functional dependence inference.

III. INFERENCE OF FUNCTIONAL DEPENDENCE IN MODEL SYSTEMS

First, we are going to test our FF MLP-based technique to detect functional dependence in coupled chaotic model systems. For instance, let us consider a pair of coupled Rössler oscillators which is a classical nonlinear model for the study of synchronous behavior, namely, GS,[12,21,35]

$$\begin{aligned} \dot{x}_{1,2} &= -\omega_{1,2}y_{1,2} - z_{1,2} + \varepsilon_{1,2}\,(x_{2,1} - x_{1,2}), \\ \dot{y}_{1,2} &= \omega_{1,2}x_{1,2} + ay_{1,2}, \quad \dot{z}_{1,2} = p + z_{1,2}\,(x_{1,2} - c), \end{aligned} \tag{4}$$

where $\mathbf{u}_{1,2} = (x_{1,2}, y_{1,2}, z_{1,2})^T$ are the vector states of interacting Rössler oscillators. The control parameters $a = 0.15$, $p = 0.2$, and $c = 10$ have been set identical for both systems, while $\omega_1 = 0.99$ and $\omega_2 = 0.95$ by the analogy with Refs. 14 and 35. In the case of unidirectional coupling, we suggest that master oscillator 1 drives response oscillator 2 and, therefore, $\varepsilon_1 = 0$ and $\varepsilon_2 = \varepsilon$. In the case of mutual coupling, parameter $\varepsilon_{1,2} = \varepsilon$ stands for the coupling strength.

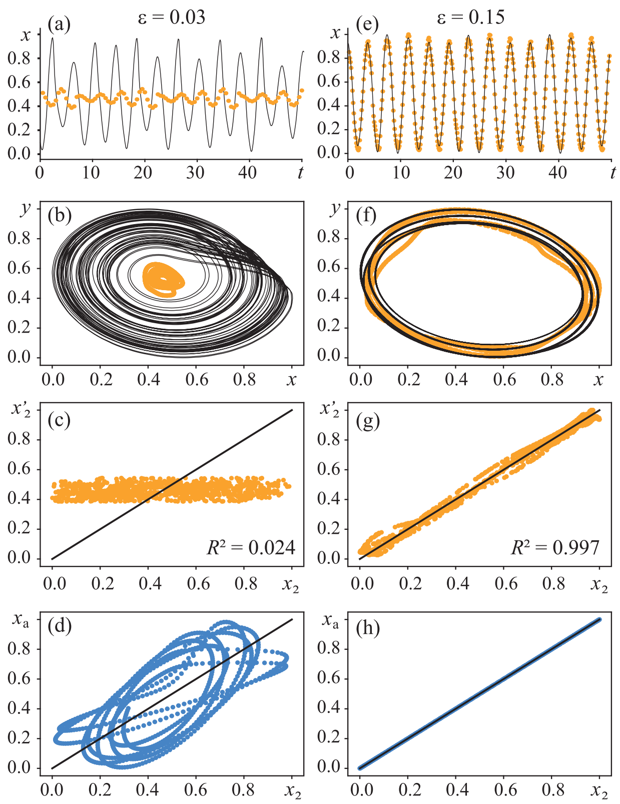

FIG. 2. Inference of functional dependence in unidirectionally coupled Rössler oscillators below ($\varepsilon = 0.03$, left column) and above ($\varepsilon = 0.15$, right column) GS threshold $\varepsilon_{GS} \approx 0.11$.[35] (a) and (e) Test sample of response Rössler oscillator time series x_2 (black curve) and its prediction x'_2 via ANN (orange points). (b) and (f) Phase portraits of response oscillator on the plane (x_2,y_2) (black) and its prediction by ANN (x'_2, y'_2) (orange). (c) and (g) Regression analysis of x_2 variable prediction by ANN model. (d) and (h) Dependence of auxiliary oscillator state x_a on response oscillator state x_2 performing verification of functional dependence between drive and response oscillators.

Figure 2 illustrates the recognition of functional dependence between unidirectionally coupled Rössler oscillators by means of the proposed FF ANN-based approach. Due to 3D phase spaces of drive and response systems, we have used MLP with 3 inputs and 3 outputs corresponding to 3 variables $(x_{1,2}, y_{1,2}, z_{1,2})$. For the training process of the MLP, we selected time intervals with a duration of 100 (10^5 samples) after long transient processes. Entire data set 10^5 pairs of $(\mathbf{u}_1, \mathbf{u}_2)$ has been randomly separated in half into training and validation sets, each consisting of 5×10^4 pairs. As the input data of MLP, we considered the drive system states $\mathbf{u}_1(t_i)$ from the training set and as the target data the corresponding response system states $\mathbf{u}_2(t_i)$.

To verify the proposed ANN-based approach and reveal GS regime in the case of unidirectional coupling, we have also used the traditional auxiliary system approach.[21] Along with response system $\mathbf{u}_2$, we also consider auxiliary system $\mathbf{u}_a = (x_a, y_a, z_a)^T$ having the same a, p, c, and $\omega_a = \omega_2$ but starting from different initial conditions. According to this method, the presence of functional dependence is detected if $\mathbf{u}_a = \mathbf{u}_2$.

The left column in Fig. 2 shows the dynamics of response Rössler system and its ANN prediction in the absence of functional relation between drive and response oscillators. Here, coupling strength $\varepsilon = 0.03$ is chosen below the GS threshold $\varepsilon_{GS} \approx 0.11$ as known from Ref. 35. It is seen that ANN fails to identify any functional relation between coupled systems and provides completely inaccurate prediction of both time series $x_2(t)$ and phase trajectory of the response oscillator [Figs. 2(a) and 2(b)]. Regression analysis also evidences that predicted and original data are completely uncorrelated with $R^2 = 0.024$ [Fig. 2(c)]. The absence of functional relation revealed by ANN is also verified via the auxiliary system approach. As seen from Fig. 2(d), the auxiliary system state is not equal to a response one $\mathbf{u}_a(t) \neq \mathbf{u}_2(t)$. By contrast, above GS threshold $\varepsilon = 0.15 > \varepsilon_{GS}$ ANN demonstrates precise enough prediction of response Rössler system with $R^2 = 0.997$ [Figs. 2(e)–2(g)]. This identifies the presence of functional dependence between the states of coupled systems, which is in agreement with the results of the auxiliary system approach [Fig. 2(h)].

We note that similar results are obtained in the case of mutually coupled Rössler systems (Fig. 3). According to the implicit-function theorem, we can consider Eq. (2) as the definition of the implicit functional relation between coupled system states, and, therefore, locally, the implicit definition of the functional relation between system states may be used, i.e., in our case of mutually coupled systems (4), $\mathbf{u}_1(t) = \tilde{\mathbf{F}}(\mathbf{u}_2(t))$ or $\mathbf{u}_2(t) = \tilde{\mathbf{F}}(\mathbf{u}_1(t))$. Taking into account these remarks, we can apply the previous FF ANN-based approach to detect the GS regime for mutual coupling using the same training procedure for ANN. By the analogy with previously considered case, ANN accurately detects the absence of functional interdependence below the GS threshold (left column in Fig. 3) and its presence above the GS threshold (right column in Fig. 3) with $R^2 = 0.183$ and $R^2 = 0.997$, respectively.

The presented results show that ANN perfectly provides functional connectivity analysis in model systems with $R^2 \approx 1$ in the case of the established functional relation and $R^2 \approx 0$ in its absence, according to R^2-score definition [Eq. (3)]. However, applying the ANN approach to an experimentally obtained data set one should take into account the presence of noise, which can essentially lower the accuracy of ANN prediction. So, let us consider the influence of noise level on ANN prediction by adding a noisy component to a generated model data in a following form: $\mathbf{u}_{1,2}(t_i) = \mathbf{u}_{1,2}(t_i) + D_0\xi_{1,2}$, where $\xi_{1,2}$ are statistically independent stochastic Gaussian processes with zero mean, and parameter D_0 defines the intensity of the noise. As one could expect, the increase in the noise level reduces the accuracy of ANN prediction quantified by the R^2-score [Fig. 4(a)]. It also results in growing variance of $x'_2(x_2)$ regression [Figs. 4(b)–4(d)]. Despite that, even at a substantial level of noise $D_0 = 0.3$, ANN prediction is still characterized by sufficiently high value of coefficient of determination $R^2 \approx 0.7$.

We can conclude that the developed FF ANN-based approach is suitable for GS detection in model systems and noisy data. In Sec. IV, we discuss the application of the developed ANN-based approach to

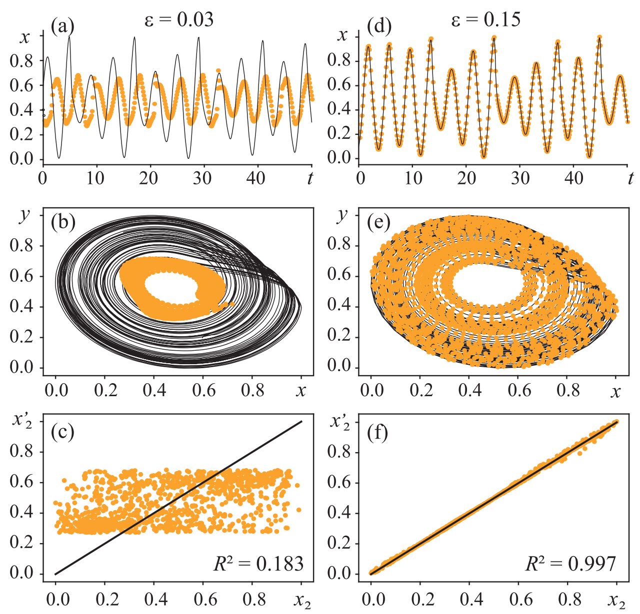

FIG. 3. Inference of functional dependence in mutually coupled Rössler oscillators below ($\varepsilon = 0.03$, left column) and above ($\varepsilon = 0.15$, right column) GS threshold $\varepsilon_{GS} \approx 0.12$.[14] (a) and (d) Test sample of the second Rössler oscillator time series x_2 (black curve) and its prediction x'_2 via ANN (orange points). (b) and (e) Phase portraits of the second oscillator on the plane (x_2,y_2) (black) and its prediction by ANN (x'_2, y'_2) (orange points). (c) and (f) Regression analysis of x_2 variable prediction by the ANN model.

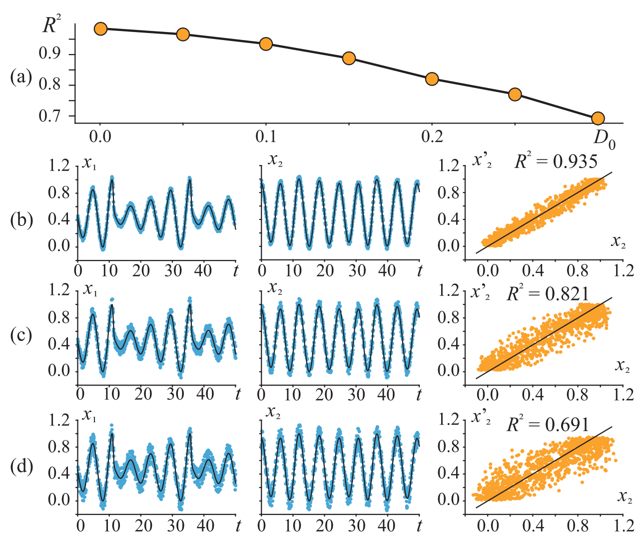

FIG. 4. Influence of noise on ANN prediction accuracy in the case of functional relationship between unidirectionally coupled Rössler oscillators ($\varepsilon = 0.15$). (a) Coefficient of determination R^2 vs noise level ξ. (b)–(d) Original (black) and noisy (blue dots) time series of drive $x_1(t)$ (left column) and response $x_2(t)$ (middle column) systems. Right column presents the results of regression analysis. Here, noise intensity takes the following values: (b) $D_0 = 0.1$, (c) 0.2, and (d) 0.3.

reveal functional connectivity from experimental neurophysiological data recorded from rodents with a genetic predisposition to absence epilepsy.

IV. APPLICATION TO ECOG DATA SET OF EPILEPTIC BRAIN

Spike-wave discharges (SWDs) are the hallmarks of absence epilepsy highly pronounced recordings of electrical brain activity and manifested as hypersynchronuous activity within cortico-thalamo-cortical network.[36] Thus, consideration of SWDs is extremely useful for the verification of the proposed method for functional connectivity inference from experimental time series. We analyzed a multichannel set of ECoG recordings taken from Wistar Albino Glaxo from Rijswijk (WAG/Rij) rats—a genetic animal model giving rise to spontaneous absence seizures.[37] In the experiments, 6 month old WAG/Rij rats were, under deep isoflorane anesthesia, chronically implanted with stainless steel electrodes in layer 4 to 6 of the somatosensory cortex (ctx4–6), as well as in the (i) posterior (PO), (ii) ventral-postero-medial (VPM), and (iii) anterior thalamic nucleus (ANT), respectively. Two weeks after surgery, ECoG signals were recorded from these structures in freely moving animals. Signals were filtered by a band pass filter with cut-off points at 1 (HP) and 100 (LP) and a 50 Hz Notch filter and digitized by WINDAQ-recording-system (DATAQ-Instruments Inc., Akron, OH) with a constant sampling rate of 2048 Hz. Experiments were carried out in accordance with the Ethical Committee on Animal Experimentation of University of Münster.

Let us consider the example of typical functional dependence emergence during epileptic discharge initiation. Figure 5(a) illustrates the typical ECoG signals recorded in cortical layer ctx6 and thalamic nucleus ANT before and during SWD onset. According to the described approach, to infer functional dependence between ctx6 and ANT we try to predict the brain state in ANT area based on one in the ctx6 area using the FF ANN. With this goal in mind, we also estimated the parameters of the embedding space of the experimental signals using mutual information approach[38] to determine the delay time τ and the false nearest neighbor method[39] to determine the embedding dimension D. We obtained the following values $\tau = 10$ ms and $D = 5$ for both signals. Thus, the architecture of MLP is such that it contains 5 inputs and 5 outputs. We have considered the emergence of functional dependence between ctx6 and ANT in a floating 1-s window, inside which we have calculated the R^2-score Fig. 5(b). One can see that the SWD onset is accompanied by an increase of R^2-score over the threshold value of 0.5 and, therefore, the establishment of a functional relationship between ctx6 and

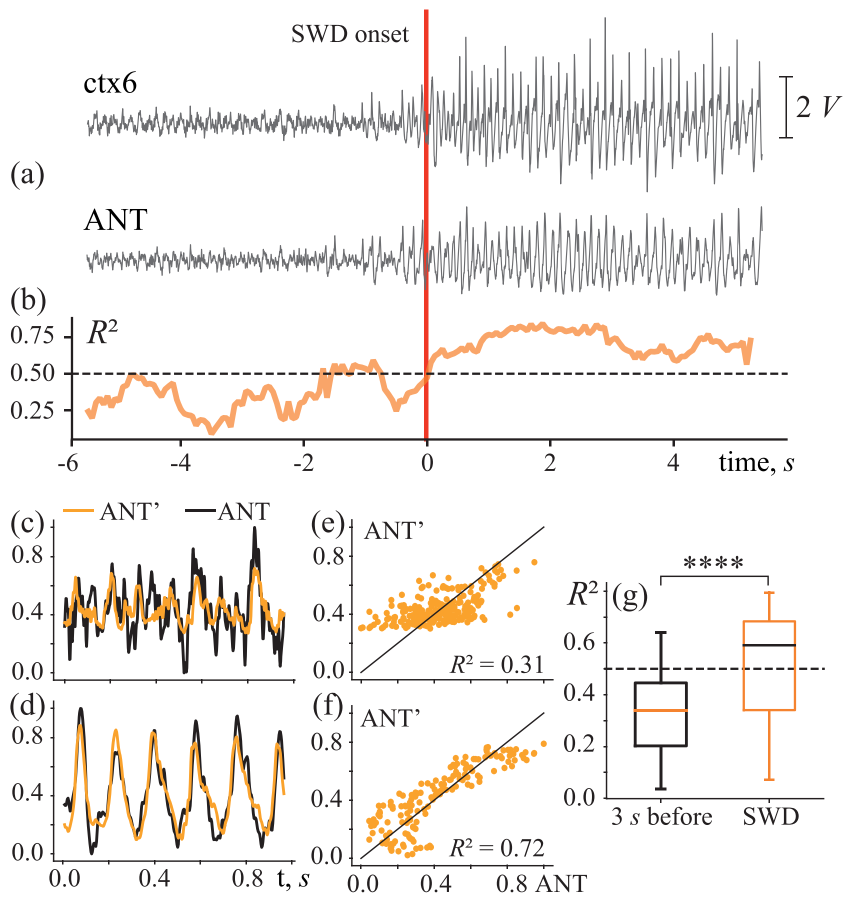

FIG. 5. (a) Typical ECoG signals recorded in cortical layer ctx6 and thalamic nucleus ANT of epileptic rat's brain including SWD beginning. (b) R^2-score computed in a floating 1-s window. Illustrations of ANT signal predictability 3 s before (c) and during SWD onset (d). Plots (e) and (f) present results of regression analysis for (c) and (d). (g) Comparison of R^2-scores computed 3 s before and during SWD onset over 20 seizure trials collected over 5 rats ($p < 0.0001$ via Wilcoxon signed-rank test for related samples). Dashed line in (b) and (e) defines R^2 threshold level of 0.5.

ANT. Figures 5(c) and 5(d) present an illustration of the possibility to predict ANT signal from the ctx6 signal in a 1-s interval during the background activity and the beginning of SWD, respectively. It is clearly seen from regression analysis in Figs. 5(e) and 5(f) that the background activity is characterized by low prediction accuracy, while the pathological epileptic activity is characterized by a high R^2-score value.

This trend is observed for all analyzed rats. Figure 5(g) shows the comparison of R^2-score averaged over the 40 trials of background and epileptic activity, collected from 6 different rats. There is a significant difference between two samples of R^2-scores, confirmed by the Wilcoxon signed-rank test for related samples ($p < 0.0001$). Besides, one can see that median value of R^2-score during seizure onset exceeds the threshold value of 0.5. Thus, we conclude that functional link between ctx6 and ANT areas emerges in all the considered rats.

Based on the considered approach for functional connectivity diagnostics in experimental time series identified on a pair of ECoG channels, we have reconstructed the structure of functional links in the thalamo-cortical network during background (3 s prior SWD onset) and pathological (1 s after SWD onset) activity shown in Fig. 6. One can see that during the background activity [Figs. 6(a) and 6(c)], the thalamic nuclei and cortical layers are not related to each other by functional relationships, but only intracortical (ctx4–ctx5, ctx5–ctx6) and intrathalamic (ANT–PO, ANT–VPM, PO–VPM) connections are observed. At the same time, the pathological activity shown in Figs. 6(b) and 6(d) is accompanied primarily by the increase of functional dependence between the thalamic nuclei and cortical layers along with a significant increase of intrathalamic connectivity [orange lines in Fig. 6(d)].

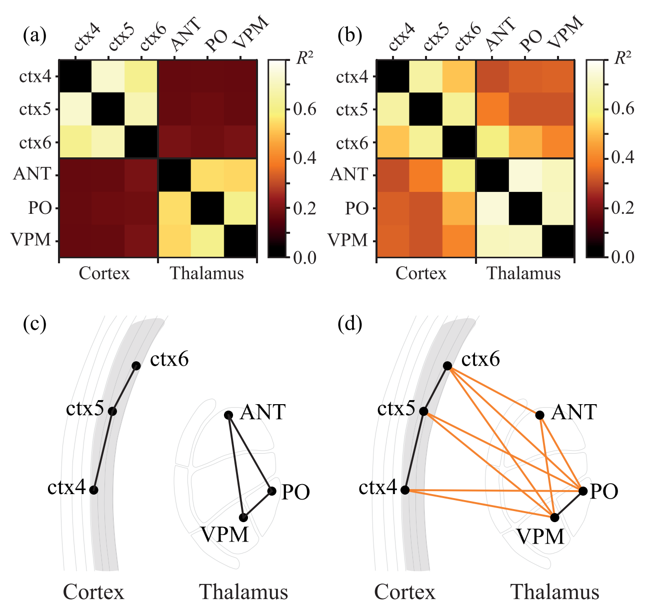

FIG. 6. Functional connectivity matrices in cortico-thalamo-cortical epileptic brain network reconstructed via the FF ANN-based approach (a) 3 s before and (b) 1 s after SWD onset over all 6 participated animals, and corresponding network representations (c) and (d). Here, black lines indicate emergent functional links, whereas orange lines highlight links with significantly increasing R^2-score (confirmed by Wilcoxon signed-rank test with Bonferroni correction). Each link is characterized by a median value of R^2-score.

V. CONCLUSION

In conclusion, we have proposed a machine learning based method for detecting functional connectivity in unidirectionally and mutually coupled systems without additional information about analyzed systems. We show for the first time that feed-forward ANN (e.g., MLP) with nonlinear units is efficient in inference of functional dependence between considered systems. We apply a novel approach to the chaotic Rössler system and demonstrate good agreement with the previous well-known results in GS studies. Then, we use our method to predict the functional network of an epileptic brain based on ECoG data set of WAG/Rij rat with genetic predisposition to absence epilepsy. We show the formation of functional relations between cortical layers and thalamic nuclei after the onset of an epileptic discharge. The developed feed-forward ANN method which does not require large computational costs and which is able to work with short data trials contribute to methods of analysis and prediction of connectivity in multichannel experimental data of different nature (e.g., biological, neurophysiological, climate, big data sets, etc.).

ACKNOWLEDGMENTS

This work was supported by the Russian Science Foundation (Grant No. 17-72-30003).

REFERENCES

[1] D. S. Bassett and O. Sporns, "Network neuroscience," Nat. Neurosci. **20**, 353–364 (2017).
[2] S. F. Muldoon, E. W. Bridgeford, and D. S. Bassett, "Small-world propensity and weighted brain networks," Sci. Rep. **6**, 22057 (2016).
[3] A. Zhigalov, G. Arnulfo, L. Nobili, S. Palva, and J. M. Palva, "Modular co-organization of functional connectivity and scale-free dynamics in the human brain," Netw. Neurosci. **1**, 143–165 (2017).
[4] A. Schnitzler and J. Gross, "Normal and pathological oscillatory communication in the brain," Nat. Rev. Neurosci. **6**, 285 (2005).
[5] P. Fries, "Rhythms for cognition: Communication through coherence," Neuron **88**, 220–235 (2015).
[6] V. A. Maksimenko, A. Lüttjohann, V. V. Makarov, M. V. Goremyko, A. A. Koronovskii, V. Nedaivozov, A. E. Runnova, G. Luijtelaar van, A. E. Hramov, and S. Boccaletti, "Macroscopic and microscopic spectral properties of brain networks during local and global synchronization," Phys. Rev. E **96**, 12316 (2017).
[7] V. A. Maksimenko, A. E. Runnova, N. S. Frolov, V. V. Makarov, V. O. Nedaivozov, A. A. Koronovskii, A. N. Pisarchik, and A. E. Hramov, "Multiscale neural connectivity during human sensory processing in the brain," Phys. Rev. E **97**, 052405 (2018).
[8] V. V. Makarov, M. O. Zhuravlev, A. E. Runnova, P. Protasov, V. A. Maksimenko, N. S. Frolov, A. N. Pisarchik, and A. E. Hramov, "Betweenness centrality in multiplex brain network during mental task evaluation," Phys. Rev. E **98**, 62413 (2018).
[9] A. Lüttjohann and G. van Luijtelaar, "Dynamics of networks during absence seizure's on-and offset in rodents and man," Front. Physiol. **6**, 16 (2015).
[10] C. J. Stam, "Modern network science of neurological disorders," Nat. Rev. Neurosci. **15**, 683 (2014).
[11] A. M. Bastos and J.-M. Schoffelen, "A tutorial review of functional connectivity analysis methods and their interpretational pitfalls," Front. Syst. Neurosci. **9**, 175 (2016).

[12] N. F. Rulkov, M. M. Sushchik, L. S. Tsimring, and H. D. Abarbanel, "Generalized synchronization of chaos in directionally coupled chaotic systems," Phys. Rev. E **51**, 980 (1995).
[13] A. Pikovsky, M. Rosenblum, and J. Kurths, *Synchronization: A Universal Concept in Nonlinear Sciences* (Cambridge University Press, 2003), Vol. 12.
[14] O. I. Moskalenko, A. A. Koronovskii, A. E. Hramov, and S. Boccaletti, "Generalized synchronization in mutually coupled oscillators and complex networks," Phys. Rev. E **86**, 036216 (2012).
[15] L. M. Pecora and T. L. Carroll, "Synchronization of chaotic systems," Chaos **25**, 097611 (2015).
[16] A. N. Pisarchik and F. R. Ruiz-Oliveras, "Optical chaotic communication using generalized and complete synchronization," IEEE J. Quantum Electron. **46**, 279–284 (2010).
[17] A. A. Koronovskii, O. I. Moskalenko, and A. E. Hramov, "On the use of chaotic synchronization for secure communication," Phys.-Usp. **52**, 1213 (2009).
[18] M. Prokhorov, V. Ponomarenko, D. Kulminskiy, A. Koronovskii, O. Moskalenko, and A. Hramov, "Resistant to noise chaotic communication scheme exploiting the regime of generalized synchronization," Nonlinear Dyn. **87**, 2039–2050 (2017).
[19] M. X. Cohen, *Analyzing Neural Time Series Data: Theory and Practice* (MIT Press, 2014).
[20] A. E. Hramov, V. A. Maksimenko, S. V. Pchelintseva, A. E. Runnova, V. V. Grubov, V. Y. Musatov, M. O. Zhuravlev, A. A. Koronovskii, and A. N. Pisarchik, "Classifying the perceptual interpretations of a bistable image using EEG and artificial neural networks," Front. Neurosci. **11**, 674 (2017).
[21] H. D. Abarbanel, N. F. Rulkov, and M. M. Sushchik, "Generalized synchronization of chaos: The auxiliary system approach," Phys. Rev. E **53**, 4528 (1996).
[22] K. Pyragas, "Weak and strong synchronization of chaos," Phys. Rev. E **54**, R4508 (1996).
[23] A. A. Koronovskii, O. I. Moskalenko, and A. E. Hramov, "Nearest neighbors, phase tubes, and generalized synchronization," Phys. Rev. E **84**, 037201 (2011).
[24] B. Lusch, J. N. Kutz, and S. L. Brunton, "Deep learning for universal linear embeddings of nonlinear dynamics," Nat. Commun. **9**, 4950 (2018).
[25] T. Weng, H. Yang, C. Gu, J. Zhang, and M. Small, "Synchronization of chaotic systems and their machine-learning models," Phys. Rev. E **99**, 042203 (2019).
[26] J. Pathak, B. Hunt, M. Girvan, Z. Lu, and E. Ott, "Model-free prediction of large spatiotemporally chaotic systems from data: A reservoir computing approach," Phys. Rev. Lett. **120**, 024102 (2018).
[27] J. Pathak, Z. Lu, B. R. Hunt, M. Girvan, and E. Ott, "Using machine learning to replicate chaotic attractors and calculate Lyapunov exponents from data," Chaos **27**, 121102 (2017).
[28] Z. Lu, B. R. Hunt, and E. Ott, "Attractor reconstruction by machine learning," Chaos **28**, 061104 (2018).
[29] A. E. Hramov, N. S. Frolov, V. A. Maksimenko, V. V. Makarov, A. A. Koronovskii, J. Garcia-Prieto, L. F. Antón-Toro, F. Maestú, and A. N. Pisarchik, "Artificial neural network detects human uncertainty," Chaos **28**, 033607 (2018).
[30] D. Ibáñez-Soria, J. Garcia-Ojalvo, A. Soria-Frisch, and G. Ruffini, "Detection of generalized synchronization using echo state networks," Chaos **28**, 033118 (2018).
[31] K. Hornik, M. Stinchcombe, and H. White, "Multilayer feedforward networks are universal approximators," Neural Netw. **2**, 359–366 (1989).
[32] G. Cybenko, "Approximation by superpositions of a sigmoidal function," Math. Control Signals Syst. **2**, 303–314 (1989).
[33] I. Goodfellow, Y. Bengio, and A. Courville, "Deep feedforward networks," in *Deep Learning* (MIT Press, 2016), pp. 168–227.
[34] F. Chollet *et al.*, See https://keras.io for "Keras" (2015).
[35] A. E. Hramov and A. A. Koronovskii, "Generalized synchronization: A modified system approach," Phys. Rev. E **71**, 067201 (2005).
[36] E. Sitnikova, "Thalamo-cortical mechanisms of sleep spindles and spike–wave discharges in rat model of absence epilepsy (a review)," Epilepsy Res. **89**, 17–26 (2010).
[37] A. Coenen and E. Van Luijtelaar, "Genetic animal models for absence epilepsy: A review of the WAG/Rij strain of rats," Behav. Genet. **33**, 635–655 (2003).
[38] M. S. Roulston, "Estimating the errors on measured entropy and mutual information," Physica D **125**, 285–294 (1999).
[39] M. B. Kennel, R. Brown, and H. D. Abarbanel, "Determining embedding dimension for phase-space reconstruction using a geometrical construction," Phys. Rev. A **45**, 3403 (1992).